

Superconducting and pseudogap phases from scaling near a Van Hove singularity

J. González

Instituto de Estructura de la Materia. Consejo Superior de Investigaciones Científicas. Serrano 123, 28006 Madrid. Spain.
(October 27, 2018)

We study the quantum corrections to the Fermi energy of a two-dimensional electron system, showing that it is attracted towards the Van Hove singularity for a certain range of doping levels. The scaling of the Fermi level allows to cure the infrared singularities left in the BCS channel after renormalization of the leading logarithm near the divergent density of states. A phase of d -wave superconductivity arises beyond the point of optimal doping corresponding to the peak of the superconducting instability. For lower doping levels, the condensation of particle-hole pairs due to the nesting of the saddle points takes over, leading to the opening of a gap for quasiparticles in the neighborhood of the singular points.

71.10.Hf, 71.10.-w, 74.20.Mn

The study of the electronic properties of the cuprates represents nowadays a great challenge from the theoretical point of view, as the phenomenology of these materials has become increasingly rich during the last decade. There have only been a few attempts to develop a theory that may encompass the main experimental features [1], including the antiferromagnetism of the undoped compounds and the pseudogap phase above the superconducting transition. Additionally, other proposals have focused on the mechanism of superconductivity, stressing the role played by antiferromagnetic fluctuations [2] or by the proximity to a Van Hove singularity (VHS) in the doped materials [3].

The later approach has received much attention recently, since it establishes a natural competition between magnetic and superconducting instabilities in a two-dimensional (2D) system [4–8]. The investigation of the model of electrons near a VHS is delicate due to the appearance of logarithmic divergences in perturbation theory. In a renormalization group (RG) framework, one has to handle infrared singularities which arise after renormalizing away the leading logarithm, as the energy dependence of some quantities comes in powers of a logarithm square [9].

Most part of the analyses of the problem have been made fixing the Fermi level at the VHS from the start. This questions the naturalness of the predicted instabilities, that rely critically on the proximity to the singular density of states. The Fermi energy is actually a dynamical quantity that is shifted by quantum corrections. It has been shown that the VHS has the tendency to attract the Fermi level of the electron system [10–13]. It is therefore more appropriate to let the chemical potential free to evolve as the states are integrated in the quantum theory. This also solves at once the problem of the infrared divergences, as the shift of the chemical potential from the VHS acts as an infrared cutoff in the logarithmic dependences left in the renormalization.

We illustrate the above ideas in the case of the $t - t'$ Hubbard model, which has a dispersion relation with saddle points at $A = (\pi, 0)$ and $B = (0, \pi)$. We deal with a wilsonian RG approach in which the chemical potential

μ is originally placed away from the VHS, and electron modes in two thin slices about energies $\mu + \Lambda$ and $\mu - \Lambda$ are progressively integrated out [14]. At each RG step, the chemical potential is free to reacomodate due to the self-energy corrections from the charge integrated out.

The behavior of μ as $\Lambda \rightarrow 0$ can be obtained by solving the frequency and momentum-independent part of the Schwinger-Dyson equation $1/G = 1/G_0 - \Sigma$. The charge in the slice $d\Lambda$ is given in terms of the density of states $n(\varepsilon)$ by $n(\mu - \Lambda)d\Lambda$. It couples through the forward-scattering vertex F in the usual Hartree and exchange diagrams. To improve the perturbative approach, one has to take into account that F is also a scale-dependent quantity [6], whose value vanishes in the proximity to the VHS according to the expression $F(\varepsilon) \approx F_0/(1 - F_0 \log(\varepsilon)/(4\pi^2 t))$. Thus, upon integration of high-energy modes in a thin slice $d\Lambda$, the chemical potential μ is shifted according to

$$\frac{d\mu}{d\Lambda} = F(\mu/(\mu - \Lambda)) n(\mu - \Lambda) \quad (1)$$

The differential renormalization given by Eq. (1) leads to the scaling of μ as a function of Λ . It can be seen that, in a certain range, the flow of the chemical potential is attracted by the VHS as $\Lambda \rightarrow 0$. If F were constant, the fixed-point condition $-1 + F n(\tilde{\mu}) = 0$, with $\tilde{\mu} = \mu - \Lambda$, would give $\mu(\Lambda)$. Taking into account the scaling of the F vertex, it is found that the renormalized value of μ lies very close to to the level of the singularity, for appropriate values of the bare chemical potential.

We have represented in Fig. 1 the results of solving the scaling equation with a model density of states $n(\varepsilon) = \log(t/|\varepsilon|)/(4\pi^2 t)$ for $|\varepsilon| \leq 0.5t$, and constant elsewhere. We observe that there is a range of nominal values of the chemical potential in which this is attracted towards the VHS. As a consequence of that, there is a range of filling levels that are forbidden above the level of the singularity.

In an open system, the pinning of the Fermi level to the VHS can be realized by exchanging particles with the environment, as greater stability is attained then in the system [13]. In a closed system, however, the mechanism of pinning can be only realized if the Fermi line deforms

to become closer to the saddle points of the dispersion relation. This is consistent with the renormalization of the Fermi line observed in numerical studies of the Hubbard model, which is translated into a shift of the next-to-nearest-neighbor hopping t' [15,16]. Such an effect is also in agreement with recent experimental observations reported in Ref. [17]. It has been shown there that the Fermi line of Bi-2212 bends progressively as the doping level is increased, so that even in the overdoped regime it does not lose its hole-like character.

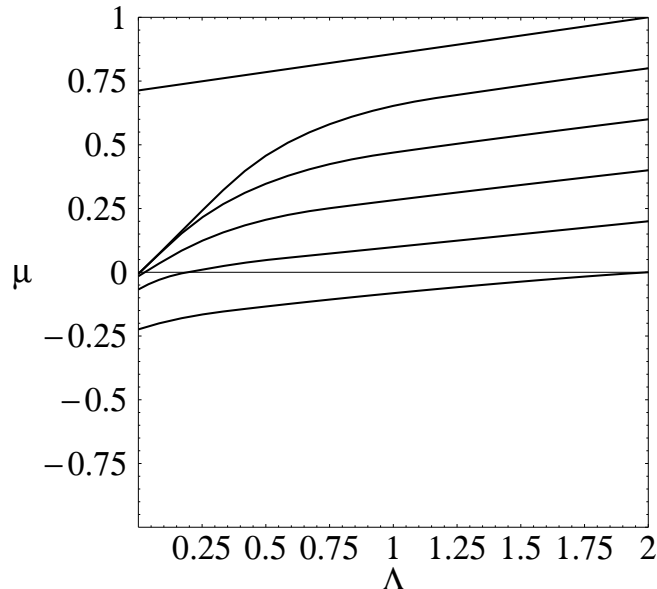


FIG. 1. Scaling of the chemical potential as a function of the high-energy cutoff. The results correspond to the Hubbard coupling $U = 4t$.

The scaling of the chemical potential $\mu(\Lambda)$ towards the VHS triggers the different instabilities in the system. These can be traced back to the divergent behavior of some of the interaction channels. Among all the kinematics, two different channels develop a singularity for an imaginary value of the frequency, namely the BCS channel of colliding particles with zero total momentum and the channel with momentum transfer $\mathbf{Q} \equiv (\pi, \pi)$. Such features are related to a phenomenon of condensation and the opening of new phases, while the singularities in the rest of the channels arise for real values of the frequency and they correspond to the appearance of new excited states.

In what follows, we concentrate on the renormalization of the vertices with BCS kinematics, listed in Fig. 2, and of those with momentum transfer $\mathbf{Q} \equiv (\pi, \pi)$, listed in Fig. 3. In a wilsonian RG approach of the kind developed in Ref. [14], processes with the latter kinematics are disentangled from the divergences in the BCS channel, at least at the one-loop level. This holds in particular for a saddle-point dispersion relation since, for kinematics in which the total momentum of the incoming particles is not precisely zero, particle-particle diagrams give irrele-

vant contributions $\sim (d\Lambda)^2$ at each RG step [14].

The converse statement is also true, and the vertices with the BCS kinematics V_{intra} and V_{umk} only get renormalized between themselves at the one-loop level. This comes from the fact that the integration of modes in the differential slices of energy $\pm\Lambda$ only produces contributions of order $\sim d\Lambda$ through particle-particle corrections to the above mentioned vertices [14]. The scaling equations for V_{intra} and V_{umk} take the form

$$\Lambda \frac{\partial V_{intra}}{\partial \Lambda} = c n(\mu - \Lambda) (V_{intra}^2 + V_{umk}^2) \quad (2)$$

$$\Lambda \frac{\partial V_{umk}}{\partial \Lambda} = 2c n(\mu - \Lambda) V_{intra} V_{umk} \quad (3)$$

with $c \equiv 1/\sqrt{1 - 4(t'/t)^2}$.

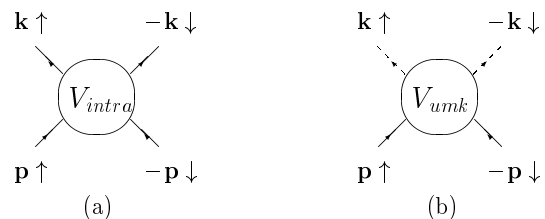


FIG. 2. BCS vertices that undergo renormalization by particle-particle diagrams. The solid and dashed lines stand for modes in the neighborhood of the two different saddle points.

If one were to take the bare coupling U of the Hubbard model as the initial point of the RG scaling, the set of Eqs. (2)-(3) would not provide interesting physics. This is so because we would have in such case $V_{intra} = V_{umk} = U$, and sending the cutoff to zero would simply reduce monotonically the interactions in these channels. However, the diagonals in this space of couplings mark the boundary between the regions of stable and unstable scaling. The slightest perturbation with $V_{intra} < V_{umk}$ will make the couplings to grow large, pointing at the appearance of new features in the system.

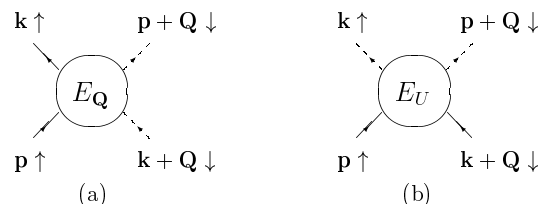


FIG. 3. Exchange and Umklapp vertices that undergo renormalization by particle-hole diagrams.

An interesting effect comes from the fact that, even in the Hubbard model, there are corrections that vanish in the low-energy limit $\Lambda \rightarrow 0$ (irrelevant operators) but may drive to the unstable regime at the early stages of the scaling. The Kohn-Luttinger effect, that leads to a pairing instability in the Fermi liquid at very low energies [18], can be established on the same grounds in the RG framework [14]. In the case of the Hubbard model, the corrections are given by the horizontal iteration of the

bubble diagrams in Fig. 4. The momentum flowing to the bubbles is not in general close to 0, in the first case, nor to \mathbf{Q} , in the second. In the wilsonian RG scheme, these particle-hole bubbles scale therefore as $\sim (d\Lambda)^2$, and they are considered irrelevant contributions [14].

In the Hubbard model with $t' < 0.276t$, the corrections coming from the iteration of diagram (a) in Fig. 4 have smaller strength than those from diagram (b) [4]. As long as these are antiscreening diagrams, i.e. they add to the bare repulsive interaction, the conditions are met to have an unstable scaling for the vertices in Fig. 2, with the above constraint on t and t' . The singular behavior develops for the combination $V_{intra} - V_{umk}$, in which the particle-particle diagrams build up a pole for an imaginary value of the frequency. The physical interpretation is that there is a condensation of Cooper pairs at the scale where the vertex function diverges [19]. The symmetry of the order parameter turns out to be d -wave, as the combination $V_{intra} - V_{umk}$ corresponds to having opposite amplitudes in the two saddle points.

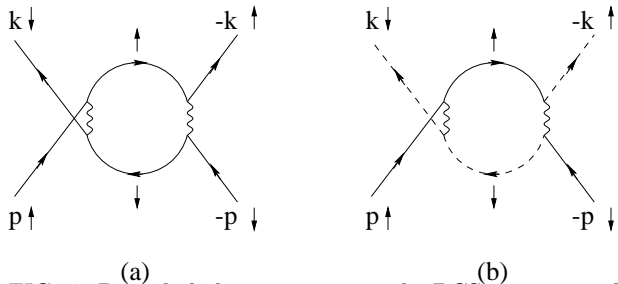


FIG. 4. Particle-hole corrections to the BCS vertices in the Hubbard model.

In our approach, the scaling of the chemical potential $\mu(\Lambda)$ regularizes the divergence of the density of states in Eqs. (2)-(3). The result of computing the scale at which $V_{intra} - V_{umk}$ diverges, for a value of the Hubbard coupling $U = 4t$, has been represented in Fig. 5. A singularity is only found for values of the bare chemical potential $\mu_0 = \mu(\Lambda_0)$ which lead to attraction of the Fermi level to the VHS. The curve of the critical scale reaches a maximum for a certain value of optimal doping, and then it decreases for smaller values of μ_0 as the chemical potential is not precisely pinned to the VHS in the low-energy limit.

The instability in the BCS channel has to be matched against the strong tendency towards a magnetic instability at wave-vector $\mathbf{Q} = (\pi, \pi)$ for $t' < 0.276t$ [4]. In the RG framework, this comes from the existence of particle-hole contributions which grow large at low energies. They are built from diagrams similar to (b) of Fig. 4, but with the momentum flowing into the bubble being precisely \mathbf{Q} . This kinematics corresponds to the vertices $E_{\mathbf{Q}}$ and E_U that we have defined in Fig. 3.

It can be seen that, at least at the one-loop level, the vertices $E_{\mathbf{Q}}$ and E_U are only renormalized by interactions with their own kinematics in the wilsonian approach. This leads to the scaling equation

$$\Lambda \frac{\partial(E_{\mathbf{Q}} + E_U)}{\partial\Lambda} = -c'(E_{\mathbf{Q}} + E_U)^2 / (4\pi^2 t) \quad (4)$$

with $c' \equiv \log \left[\left(1 + \sqrt{1 - 4(t'/t)^2} \right) / (2t'/t) \right]$. In the low-energy limit, a singularity is reached at a certain value of Λ . The logarithmically divergent particle-hole bubbles building up the singularity have an imaginary part equal to $i\pi/2$ times $c'/(4\pi^2 t)$, which means that the vertex gets actually a pole for an imaginary value of the frequency.

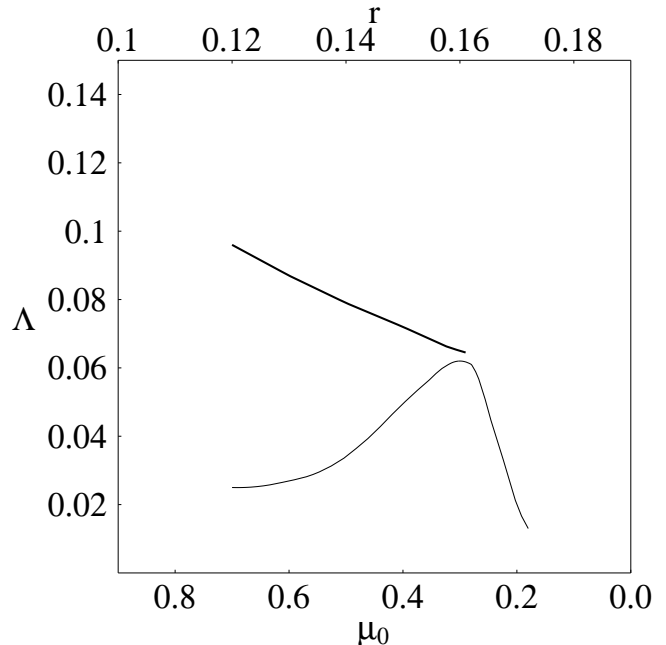


FIG. 5. Plot of the scale of the transition to the pseudogap phase (thick line) and of the superconducting instability (thin line) as a function of the bare chemical potential and $r = t'/t$.

Thus, the divergence in this channel gives rise to the condensation of particle-hole pairs with momentum \mathbf{Q} . This physical interpretation is similar to that of the superconducting instability [19], but the presence in this case of a macroscopic number of particle-hole pairs leads to nonvanishing expectation values of the type $\int d^3k \langle \Psi_{A\uparrow}^\dagger(\mathbf{k}) \Psi_{B\downarrow}(\mathbf{k} + \mathbf{Q}) \rangle \equiv \Delta$, $\Psi_{\alpha\sigma}(\mathbf{k})$ being the electron field operator at saddle point α . This has a drastic effect in the low-energy spectrum, since the electron propagator is corrected by the insertion of the condensate as shown in Fig. 6. The result is that a gap of magnitude $|\Delta|$ opens up in the spectrum of quasiparticles. The appearance of this gap takes place in the neighborhood of the saddle points, while gapless quasiparticle excitations still exist in the rest of the Fermi line not affected by the nesting of such singular points.

The point at which the vertex $E_{\mathbf{Q}} + E_U$ diverges can be estimated from Eq. (4), and it has been represented as a function of t' in Fig. 5. In accordance with the known results about the renormalization of t' with doping [16], we have assumed a variation of its effective value following the qualitative trend shown in the figure. The scale

of condensation of particle-hole pairs is larger than the scale of the superconducting instability up to the point of optimal doping marked by the peak of the latter. In this regime, the opening of a gap of magnitude $|\Delta|$ is the effect that prevails, and the renormalization of the interactions is stopped at that energy scale.

$$\overline{G}_A(\mathbf{k}) = \overline{G}_A^{(0)}(\mathbf{k}) + \overline{G}_A^{(0)}(\mathbf{k}) \overline{G}_B^{(0)}(\mathbf{k}+\mathbf{Q}) \overline{G}_A(\mathbf{k})$$

FIG. 6. Self-consistent equation for the dressed electron propagator G in the particle-hole condensate, in terms of the undressed propagators $G_A^{(0)}$ and $G_B^{(0)}$ at the two inequivalent saddle points.

On the other hand, the superconducting instability takes over beyond the optimal doping. The chemical potential departs then from the VHS at low energies, by an amount that becomes of the same order as the scale that would be predicted for the magnetic instability. In these conditions the scaling of $E_{\mathbf{Q}} + E_U$, which relies on the pinning to the VHS, is arrested before the singularity in the vertex is reached. This is in contrast to the scaling in the BCS channel given by Eqs. (2)-(3), which holds irrespective of the pinning to the VHS [14].

A closer look at the origin of the singularity in the particle-hole sector shows that it arises without a preferred direction of the spin. The divergence in the exchange channel may result in a nonvanishing expectation value with spin projection S_x or S_y , depending on the choice of the condensate wavefunction. A similar divergence in the channel with momentum transfer \mathbf{Q} and no spin-flip shows that $\int d^3k \langle \Psi_{A\uparrow}^+(\mathbf{k}) \Psi_{B\uparrow}(\mathbf{k} + \mathbf{Q}) \rangle$ has also an absolute value precisely equal to $|\Delta|$. Depending on the different combinations of phases, the spin of the condensate may point in any direction of the space, what provides a check of the rotational invariance of the wilsonian RG scheme.

When considering the model strictly at zero temperature, the ground state of the system is forced to choose a definite projection of the spin. The condensation of particle-hole pairs leads then to the spontaneous breakdown of the $SO(3)$ invariance. As a consequence, a pair of Goldstone bosons arise corresponding to spin waves on top of the condensate of particle-hole pairs. In the regime below optimal doping where the magnetic instability prevails, these are the gapless excitations of the spectrum together with the quasiparticles from the regions not affected by the nesting of the saddle points.

We have thus clarified the nature of the magnetic instability that arises when the Fermi level is pinned to the VHS of the electron system. The main physical effect is the condensation of particle-hole pairs, which results in the opening of a gap for the quasiparticles in the neighborhood of the saddle points. This is the dominant instability up to the optimal doping marked by the peak of the

scale of the superconducting instability, which takes over for higher doping levels. The properties that we have discussed rely on the existence of an attractive fixed-point in the scaling of the chemical potential of the 2D system. They are therefore robust as they do not depend on fine-tuning or on the particular details of the model, what may explain some of the universal properties of the hole-doped copper-oxide superconductors.

Fruitful discussions with F. Guinea are gratefully acknowledged. This work has been partly supported by CI-CyT (Spain) and CAM (Madrid, Spain) through grants PB96/0875 and 07N/0045/98.

-
- [1] See, for instance, E. Dagotto, *Rev. Mod. Phys.* **66**, 763 (1994), and P. W. Anderson, *The Theory of Superconductivity in the High- T_c Cuprates* (Princeton Univ., Princeton, 1997).
 - [2] N. E. Bickers, D. J. Scalapino and S. R. White, *Phys. Rev. Lett.* **62**, 961 (1989). P. Monthoux, A. V. Balatsky and D. Pines, *Phys. Rev. B* **46**, 14803 (1992).
 - [3] D. M. Newns *et al.*, *Phys. Rev. Lett.* **69**, 1264 (1992). P. C. Pattnaik, C. L. Kane, D. M. Newns and C. C. Tsuei, *Phys. Rev. B* **45**, 5714 (1992). L. B. Ioffe and A. J. Millis, *Phys. Rev. B* **54**, 3645 (1996). For a review, see R. S. Markiewicz, *J. Phys. Chem. Sol.* **58**, 1179 (1997).
 - [4] J. V. Alvarez, J. González, F. Guinea and M. A. H. Vozmediano, *J. Phys. Soc. Jpn.* **67**, 1868 (1998).
 - [5] C. J. Halboth and W. Metzner, *Phys. Rev. B* **61**, 7364 (2000); *Phys. Rev. Lett.* **85**, 5162 (2000).
 - [6] J. González, F. Guinea and M. A. H. Vozmediano, *Phys. Rev. Lett.* **84**, 4930 (2000).
 - [7] C. Honerkamp, M. Salmhofer, N. Furukawa and T. M. Rice, *Phys. Rev. B* **63** 35109 (2001).
 - [8] B. Binz, D. Baeriswyl and B. Douçot, report cond-mat/0104424.
 - [9] H. J. Schulz, *Europhys. Lett.* **4**, 609 (1987). I. E. Dzyaloshinskii, *Sov. Phys. JETP* **66**, 848 (1987).
 - [10] R. S. Markiewicz, *J. Phys.: Condens. Matter* **2**, 665 (1990).
 - [11] J. González, F. Guinea and M. A. H. Vozmediano, *Europhys. Lett.* **34**, 711 (1996); *Nucl. Phys. B* **485**, 694 (1997).
 - [12] G. Kastinakis, *Physica C* **340**, 119 (2000).
 - [13] J. González, *Phys. Rev. B* **63**, 45114 (2001).
 - [14] R. Shankar, *Rev. Mod. Phys.* **66**, 129 (1994).
 - [15] D. Duffy and A. Moreo, *Phys. Rev. B* **52**, 15607 (1995).
 - [16] A. Himeda and M. Ogata, report cond-mat/0003278.
 - [17] A. A. Kordyuk *et al.*, report cond-mat/0104294.
 - [18] W. Kohn and J. M. Luttinger, *Phys. Rev. Lett.* **15**, 524 (1965).
 - [19] A. A. Abrikosov, L. P. Gorkov and I. E. Dzyaloshinski, *Methods of Quantum Field Theory in Statistical Physics*, Chap. 7 (Dover, New York, 1975).